Detection of low-magnetic fields by rubidium (^{87}Rb) vapor cell

M. J. Maciel[1], **M. F. Silva**[1], **S. Pimenta**[1] **and J. H. Correia**[1]

[1] University of Minho, CMEMS-UMinho, Guimaraes, Portugal

mmaciel@dei.uminho.pt

Abstract. This paper describes the work carried out to assess the use of a quartz reference rubidium (^{87}Rb) vapor cell for non-invasively magnetoencephalography, avoiding cryogenically cooled sensors as the Superconducting Quantum Interference Devices (SQUIDs). An experimental setup based on a cylindrical glass vapor cell of ^{87}Rb (l = 75 mm, d = 19 mm) was developed. The ^{87}Rb cell was heated to around 75°C and it was optically pumped with polarized light (range 750-850 nm), tuned to the D1 transition of rubidium, for spin-polarization of the atoms, and the intensity of the light transmitted through the cell was detected using a photodiode. Without magnetic field, the photodiode current is maximized but when a small transverse magnetic field is present a measurable drop in light transmission occurs. A Magnetic Shielded Box (MSB) made by a nickel-iron ferromagnetic alloy, was used for nulling background magnetic fields and the transmittance light versus transverse magnetic field intensity (100-1000 nT) was measured.

1. Introduction

Biomagnetism relies on the study of weak magnetic fields generated by the biological systems, including the human body. Particularly, the magnetic field generated by the human brain is one of the most biomagnetism signals extensively investigated [1]. For example, the measurement of the magnetic fields produced by the human brain are used to diagnose epilepsy and also to study the neural response to different stimulus, as auditory and visual [2,3]. Magnetoencephalography (MEG) is the technique which allows the direct imaging of the human brain electrophysiology by measuring the magnetic fields generated at the scalp by neural currents, giving access to localized neuronal activity in the brain [2,4]. Superconducting Quantum Interference Devices (SQUIDs) are the most used technology for MEG measurements [3,5,6]. These cryogenically cooling magnetic sensors must be housed within a liquid helium draw with a vacuum space between the cooled sensors and the scalp [2].

Recently, the alkali-metal-vapor atomic magnetometers (AM) have been emerging as a promising noncryogenic alternative to SQUIDs sensors in biomagnetism measurements [3,6]. The AM technology has advanced significantly, and the laboratory AM prototypes have been demonstrated sensitivities which exceeded the ones associated to the SQUIDs magnetometers [1]. The major advantage of AM is the precise measurement of magnetic fields with instruments that do not need to be cooled to cryogenic temperatures, eliminating the need for complex cryogenic equipment, which can reduce the cost and complexity of a MEG equipment [1,4]. The physical principle of the AM relies on the measurement of the Larmor precession of spin-polarized atoms in a magnetic field. The spins form a collective moment that changes in the presence of an external magnetic field, resulting in a variation of the optical properties of the alkali-metal-vapor cell [3,6]. Therefore, the vapor cell allows the precise measurement of magnetic fields by optical spectroscopy [4]. The major advantage

of these type of magnetometers is the possibility of chip-scale microfabricated versions, allowing a reduced sensitive volume and low-cost manufacturing [1,4–9].

In this paper we present an optical setup based on a commercial rubidium cell (^{87}Rb) inside a copper solenoid coil, which generates different values of low-magnetic field. Polarized light (750-850 nm) was used as the light passing through the heated vapor cell at different magnetic field values. Section 2 presents the used magnetic and optical setup. The results and discussion are presented in section 3. Finally, section 4 contains the main conclusions and future guidelines of the proposed work.

2. Magnetic and optical setup

This section shows the theoretical approximation of the magnetic field applied to the ^{87}Rb vapor cell, according to the electrical current applied in a solenoid coil. The experimental setup for optical transmittance measurements is also presented.

2.1. Magnetic field inside a solenoid

The ^{87}Rb vapor cell (l = 75 mm, d = 19 mm, with reference GC19075-RB87 from Thorlabs) was involved in a copper solenoid coil, which generates the magnetic field. The magnetic field (B) inside the solenoid is almost uniform, and the intensity is obtained according to equation (1).

$$B = \mu \frac{N}{L} i, \tag{1}$$

where μ is the magnetic permeability inside the solenoid, N is the number of turns per unit of the length (L) and i is the current applied to the coil. Rubidium is a paramagnetic material (μ>1) and according to our estimations (based on literature [10]), μ=1.256600383×10^3 nT.m/A. The solenoid length is the length of the ^{87}Rb vapor cell used in this experiment, *i.e.*, 75 mm. N was fixed to 7, to ensure the optical transmittance measurement. Figure 1 shows the variance of the magnetic field inside the solenoid, according to the variation of the current applied to the coil (mA).

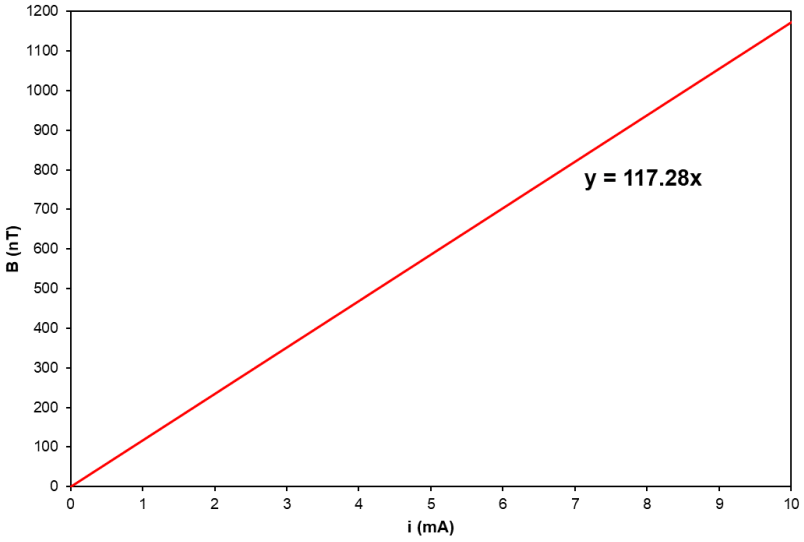

Figure 1. Magnetic field (nT) inside a solenoid with a ^{87}Rb vapor cell versus applied current to the coil (mA).

2.2. Experimental setup

The experimental setup was developed inside a custom-made Magnetic Shielded Box (MSB), to eliminate the influence of external magnetic fields. The MSB is a nickel-iron ferromagnetic alloy based in Mu-metal and used for shielding against external static or low-frequency magnetic fields. Figure 2 shows a schematic of the experimental setup. A 1.5 mm thick copper coil with 7 turns and with 75 mm of length was built at the bottom of box. A quartz reference cell of ^{87}Rb vapor was put inside of the solenoid, as can be observed in the schematic. Below the solenoid and reference vapor cell was placed a resistance heater, which reach temperatures of around 75 ºC. The MSB contains 3 apertures: the light input from optical fiber; the light output for photodetection; and an entrance for the temperature sensor. A white light source and a monochromator were used and mounted with an optical fiber and polarizer for swapping the range between 750-850 nm. A correct alignment is ensured for transmitted light intensity detection using a photodiode, which is synchronized with all the optical components for photocurrent measurement as a function of the wavelength. This configuration ensures the application of a magnetic field transversal to the light beam, which is crucial to obtain the variation of the cell transmittance as a function of the applied magnetic field.

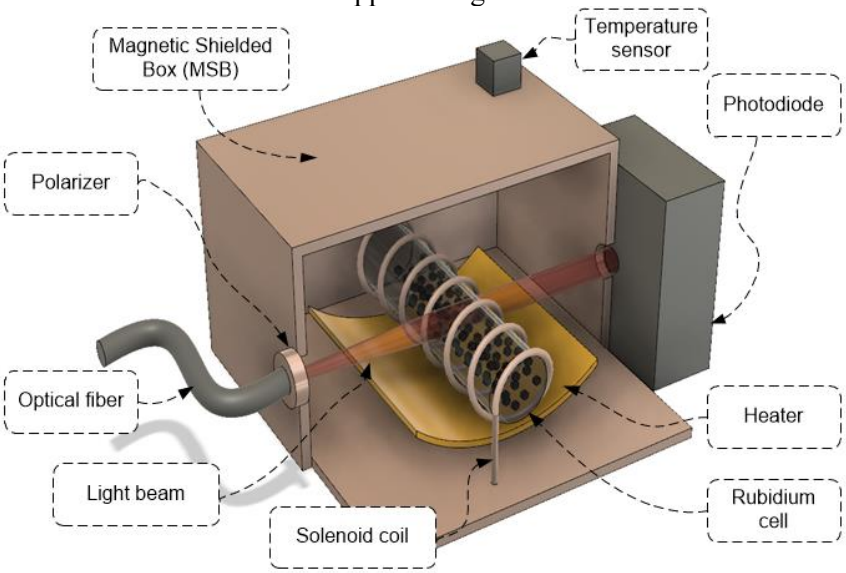

Figure 2. Schematic of the optical/magnetic setup used for optical transmittance measurement of the ^{87}Rb vapor cell according to the magnetic field applied to a solenoid coil.

A photograph of the setup is presented in Figure 3. The electrical connections of the coil and the heater were ensured by two controllers, placed at the bottom and outside the box, as can be observed in Figure 3 a). The coil controller is connected to an electrical circuit (battery charged) which causes variation in the applied current to the solenoid coil.

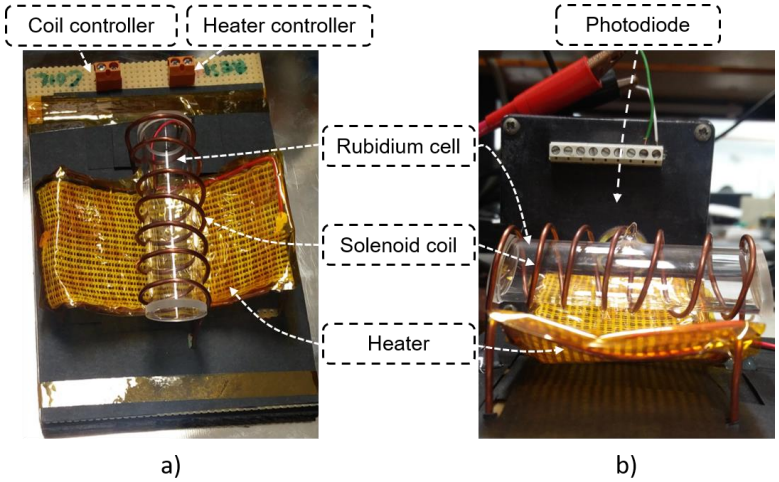

Figure 3. Photograph of the vapor cell placed in the solenoid: a) electric board, with coil and heater controllers; b) alignment of the setup with the photodiode.

3. Results and discussion

In this paper, we present the results of optical transmittance in a wavelength range between 750 nm and 850 nm. The best results were achieved in the range 780-800 nm. Particularly, we have used the 795 nm to characterize the behavior of the ^{87}Rb vapor cell, as mentioned in the literature [2,4,6,11]. Electric current was applied in the solenoid coil between 1 and 10 mA, with 1 mA increments. This variation is translated in a magnetic field intensity variation between 117 and 1173 nT (according to equation (1)). The cell was heated at a temperature of approximately 75 ºC. Initially, the reference measurement was obtained, which corresponds to the photocurrent intensity without temperature and at null magnetic field. Figure 4 presents the results of photocurrent intensity for the minimum, central and maximum magnetic fields applied to the solenoid coil. Figure 5 contains the transmittance results for the different magnetic field intensities, between 117 and 1173 nT.

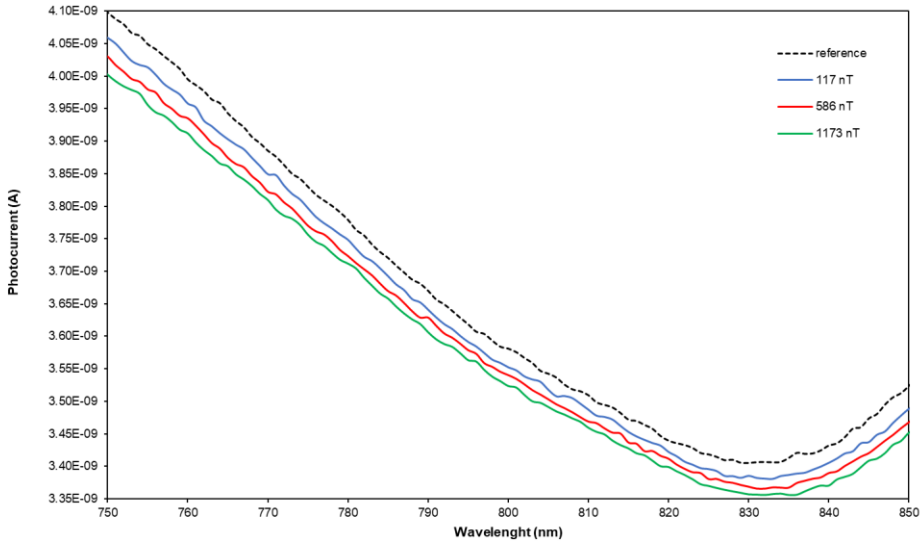

Figure 4. Photocurrent as a function of the wavelength, for different intensities of magnetic field.

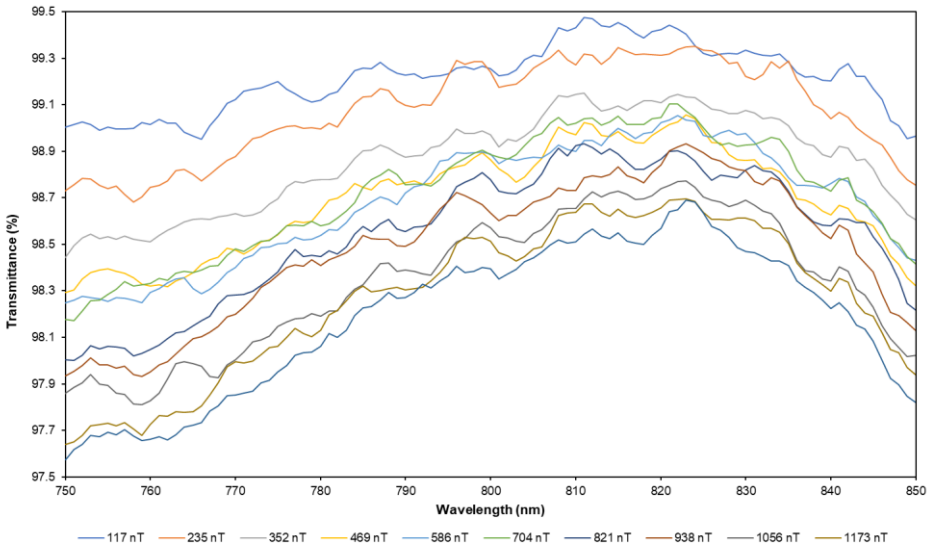

Figure 5. Optical transmittance of the ^{87}Rb vapor cell as a function of the wavelength, for different intensities of magnetic field.

The behavior of the ^{87}Rb vapor cell at 795 nm is shown in Figure 6, which represents the cell transmittance as a function of the magnetic field intensity.

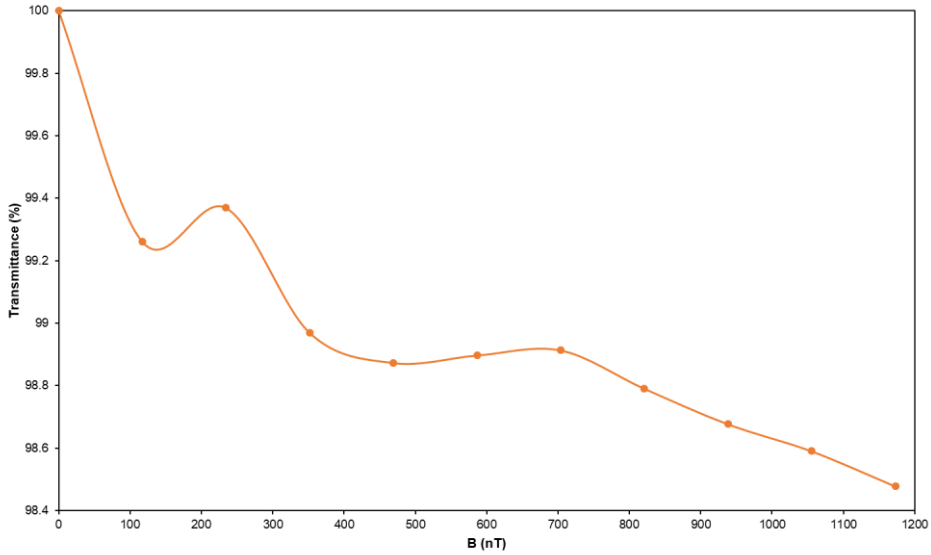

Figure 6. Optical transmittance of the ^{87}Rb vapor cell at 795 nm as a function of the magnetic field intensity.

The results clearly show a decrease in the transmittance of light of the commercial ^{87}Rb vapor cell, as the intensity of the magnetic field increases. Without the influence of magnetic field and at room temperature, the photocurrent measured in the photodiode is maximum, *i.e.*, the transmitted light through the cell is maximum. When the cell was heated, and an electrical current of 1 mA was applied, which corresponds to a magnetic field of approximately 117 nT, the optical transmittance decays to 99.26 % at the wavelength peak of 795 nm. When the magnetic field increases by a factor of 10 the transmittance value drops to 98.48 %.

4. Conclusion and future guidelines

In this paper we presented an optical and magnetic setup to measure the optical transmittance of a commercial ^{87}Rb vapor cell, from Thorlabs, as a function of the transverse magnetic field intensity applied to the cell. This setup was mounted in a custom-made magnetic shielded box, which nulls background magnetic fields. By varying the electrical current input in a solenoid coil, the magnetic field in the ^{87}Rb vapor cell varies between 117 nT and 1173 nT. When a magnetic field is applied to the ^{87}Rb vapor cell, the optical transmittance suffers a decrease proportional to the magnetic field increase. These results proved the concept of ^{87}Rb vapor cells as optimal candidates for AM.

Future guidelines include the development of micro scale vapour cell, using conventional MEMS technologies. Also, it is intended at the future work to perform measurements with lower values of transverse magnetic fields (below nT), to obtain a high sensitivity AM sensor.

Acknowledgements

This work is supported by: project MME reference 105399; FCT Strategic Project UID/EEA/04436/2019; project Infrastructures Micro&NanoFabs@PT, reference NORTE-01-0145-FEDER-022090, POR Norte, Portugal 2020; SARSPEC Lda, V.N. Gaia-Portugal; project OCT-RAMAN, PTDC/FIS-OTI/28296/2017, operation code NORTE-01-0145-FEDER-028296; and project OpticalBrain, PTDC/CTM-REF/28406/2017, operation code NORTE-01-0145-FEDER-028406.

References

[1] Shah V K and Wakai R T 2013 A compact, high performance atomic magnetometer for biomedical applications *Phys. Med. Biol.* **58** 8153–61

[2] Boto E, Holmes N, Leggett J, Roberts G, Shah V, Meyer S S, Muñoz L D, Mullinger K J, Tierney T M, Bestmann S, Barnes G R, Bowtell R and Brookes M J 2018 Moving magnetoencephalography towards real-world applications with a wearable system *Nature* **555** 657–61

[3] Kominis I K, Kornack T W, Allred J C and Romalis M V. 2003 A subfemtotesla multichannel atomic magnetometer *Lett. to Nat.* **422**

[4] Sander T H, Preusser J, Mhaskar R, Kitching J, Trahms L and Knappe S 2012 Magnetoencephalography with a chip-scale atomic magnetometer *Biomed. Opt. Express* **3** 981–90

[5] Shah V, Knappe S, Schwindt P D D and Kitching J 2007 Subpicotesla atomic magnetometry with a microfabricated vapour cell *Nat. Photonics* **1** 649–52

[6] Johnson C, Schwindt P D D and Weisend M 2010 Magnetoencephalography with a two-color pump-probe, fiber-coupled atomic magnetometer *Appl. Phys. Lett.* **97**

[7] Pétremand Y, Affolderbach C, Straessle R, Pellaton M, Briand D, Mileti G and De Rooij N F 2012 Microfabricated rubidium vapour cell with a thick glass core for small-scale atomic clock applications *J. Micromechanics Microengineering* **22** 1–8

[8] Liew L-A, Knappe S, Moreland J, Robinson H, Hollberg L and Kitching J 2004 Microfabricated alkali atom vapor cells *Appl. Phys. Lett.* **84** 2694–6

[9] Pétremand Y, Schori C, Straessle R, Mileti G, De Rooij N and Thomann P 2010 Low temperature indium-based sealing of microfabricated alkali cells for chip scale atomic clocks *EFTF 2010 - 24th European Frequency and Time Forum* pp 2–4

[10] Weast R 1984 *Handbook of Chemistry and Physics* (Boca Raton, Florida: Chemical Rubber Company Publishing.)

[11] Shah V and Romalis M V. 2009 Spin-exchange relaxation-free magnetometry using elliptically polarized light *Phys. Rev. A - At. Mol. Opt. Phys.* **80**